

We are IntechOpen, the world's leading publisher of Open Access books Built by scientists, for scientists

6,900

Open access books available

185,000

International authors and editors

200M

Downloads

Our authors are among the

154

Countries delivered to

TOP 1%

most cited scientists

12.2%

Contributors from top 500 universities



WEB OF SCIENCE™

Selection of our books indexed in the Book Citation Index
in Web of Science™ Core Collection (BKCI)

Interested in publishing with us?
Contact book.department@intechopen.com

Numbers displayed above are based on latest data collected.
For more information visit www.intechopen.com



Thermodynamic Stability and Microscopic Behavior of $\text{Ba}_x\text{Sr}_{1-x}\text{Co}_{1-y}\text{Fe}_y\text{O}_{3-\delta}$ Perovskites

Florentina Maxim, Alina Botea-Petcu, Florina Teodorescu, Ludwig J. Gauckler and Speranta Tanasescu

Abstract

The mixed conducting perovskite-type oxides $\text{Ba}_x\text{Sr}_{1-x}\text{Co}_{1-y}\text{Fe}_y\text{O}_{3-\delta}$ (BSCF) are intensively studied as potential high-performance solid oxide fuel cell cathode materials. The effect of different compositional variables and oxygen stoichiometry on the structure and thermodynamic stability of the $\text{Ba}_x\text{Sr}_{1-x}\text{Co}_{1-y}\text{Fe}_y\text{O}_{3-\delta}$ ($x = 0.2, 0.4, 0.5, 0.6, 0.8$; $y = 0.2, 0.4, 0.6, 0.8, 1$) perovskite-type compositions were investigated by solid electrolyte electrochemical cells method and scanning electron microscopy (SEM). The thermodynamic quantities represented by the partial molar free energies, enthalpies and entropies of oxygen dissolution in the perovskite phase, as well as the equilibrium partial pressures of oxygen were obtained in the temperature range of 823–1273 K. The *in situ* change of oxygen stoichiometry and the determination of thermodynamic parameters of the new oxygen-deficient BSCF compositions were studied *via* coulometric titration technique coupled with electromotive force (EMF) measurements. The effect of A- and B-site dopants concentration correlated to the variation of oxygen stoichiometry on the thermodynamic stability and morphology of the BSCF samples was evidenced.

Keywords: BSCF, perovskite-type compounds, oxygen stoichiometry, thermodynamic data, electromotive force measurements, scanning electron microscopy, cathodes SOFC

1. Introduction

The series $\text{Ba}_x\text{Sr}_{1-x}\text{Co}_{1-y}\text{Fe}_y\text{O}_{3-\delta}$ (BSCF) perovskites are well known for their good oxygen catalytic activity and mixed ionic-electronic conductivity (MIEC) and gained attention as promising electrode materials for solid oxide fuel cells (SOFCs) and oxygen-permeable membranes. Depending on temperature and oxygen partial pressure the BSCF perovskites exhibit high oxygen non-stoichiometry ($0.3 < \delta < 0.8$ at $873 < T < 1073$ K) [1–4]. This extraordinary ability to host oxygen vacancies and to transport a significant amount of oxygen anions *via* oxygen vacancies (with an oxygen diffusion coefficient of about 10^{-6} cm²/s and ionic conductivity of 0.018 S/cm at 973 K) has been reported for $\text{Ba}_{0.5}\text{Sr}_{0.5}\text{Co}_{0.8}\text{Fe}_{0.2}\text{O}_{3-\delta}$ [4–8]. However, significant differences were observed in the structural characteristics and the electrochemical performance of the BSCF solid solutions as a function of temperature (T), atmosphere (inert [9], oxidizing [10–12] and reducing [13, 14]), as well as of the nature and

concentration of A- and B-sites substituents [15–18]. As consequence, there are questions regarding the long-term stability and performance of such highly defective material under the operating conditions of an intermediate temperature solid oxide fuel cell (IT-SOFC) of 873–1073 K. At low oxygen partial pressures (under 10^{-5} atm) and in reducing conditions the structural changes through different pathways was shown [16, 17, 19]; the variation of the oxidation state of the Co ion was suggested as the driving force for these changes [14]. The formation of non-cubic phases might limit the performance of the oxygen ion conduction, by increasing the lattice stress and decreasing the oxygen vacancies mobility.

Despite the interest and the research effort in this field, many aspects of finding appropriate processing parameters and, above all, the fundamental understanding of the correlations between all the factors that ensure the optimization of the SOFC cathodes are not yet elucidated.

The aim of the study is to evidence the effect of the composition, and oxygen stoichiometry change on the thermodynamic properties and morphology of perovskite-type oxides in the $\text{Ba}_x\text{Sr}_{1-x}\text{Co}_{1-y}\text{Fe}_y\text{O}_{3-\delta}$ ($x = 0.2, 0.4, 0.5, 0.6, 0.8$; $y = 0.2, 0.4, 0.6, 0.8$ and 1) (BSCF) system. In addition, the correlative effect of temperature and defect structure on the thermodynamic behavior of the samples was discussed based on the evolution of the thermodynamic quantities of the oxygen dissolution in the perovskite structure. The partial molar thermodynamic properties of oxygen dissolution in the perovskite phase, as well the equilibrium partial pressures of oxygen have been obtained by using solid electrolyte electrochemical cells method. The influence of the oxygen stoichiometry change on the thermodynamic properties was examined using the data obtained by a coulometric titration technique coupled with EMF measurements.

2. Materials and methods

The details of the sample preparation method are presented elsewhere [13]. Briefly, powder specimens of BSCF were obtained by solid state reaction starting from barium carbonate, strontium carbonate, iron oxide and cobalt oxide raw materials. In order to reach the phase equilibrium of the desired perovskite, the powder mixture was ground and calcined for several times at 1273 K for 10 h. The X-ray diffraction analysis of the as prepared powder samples (shown elsewhere [13]) demonstrates the formation of a predominant cubic phase for all the BSCF investigated compositions, although small amounts of hexagonal phase could be present in the BSCF 8282 sample [20, 21].

The morphology of BSCF powders was analyzed by SEM using a FEI Quanta 3D equipment operated at low acceleration voltage (maximum 5 kV) and using the backscatter detector in beam deceleration mode. This SEM mode enables high resolution imaging and high surface sensitivity [22], and it was used in this study to evidence the surface features of the BSCF particles.

The electrochemical cell method was employed to obtain the thermodynamic properties of the BSCF samples. The experimental setups as well as theoretical aspects were described in detail in previous papers [23–25]. The electrochemical cell contains a yttria stabilized zirconia solid electrolyte and an iron- wüstite reference electrode:

(–) Fe, wustite/ ZrO_2 (Y_2O_3) /BSCF (+)

where BSCF denotes the $\text{Ba}_x\text{Sr}_{1-x}\text{Co}_{1-y}\text{Fe}_y\text{O}_{3-\delta}$ ($x = 0.2, 0.4, 0.5, 0.6, 0.8$; $y = 0, 0.2, 0.4, 0.6, 0.8, 1$) perovskite-type samples.

Measurements were performed in vacuum at a residual gas pressure of 10^{-5} atm. The EMF was measured with a Keithley 2000 multimeter, at 50 K intervals between

823 and 1273 K, each time waiting until equilibrium conditions were obtained. Equilibrium conditions were achieved when EMF values for increasing and decreasing temperatures agreed within ± 1 mV within a 30 minutes interval.

The solid-state coulometric titration technique was used to accurately change the oxygen stoichiometry of BSCF pellets. The titrations were performed *in situ*, in vacuum at 1123 K by using a Bi-PAD Tacussel potentiostat. The mass change $|\Delta m|$ (g) of the sample is associated to the transferred charge Q ($A \cdot s$), in agreement to Faraday's law.

$$|\Delta m| = 8.291 \cdot 10^{-5} Q \tag{1}$$

For every new composition obtained, the equilibrium EMF's values at 50 K intervals between 1073 and 1273 K are recorded in the open circuit condition.

3. Results and discussions

The BSCF samples with different cation compositions analyzed in this study are listed in **Table 1**. In order to study the effect of the A- and B- site composition of the perovskite structure on the thermodynamic properties and particles' morphologies, the samples were grouped in two sets corresponding to the variation of Ba (x) and Fe (y) concentration, respectively.

3.1 A-site effect: Ba/Sr variation

The micrographs of the as prepared BSCF powders obtained for increasing Ba content, a) $x = 0.2$, b) $x = 0.4$, c) $x = 0.5$, d) $x = 0.6$ and e) $x = 0.8$ are presented in **Figure 1**. There are two categories of morphologies specific to different compositions analyzed in this study. The first type is the well-defined particles with similar shape and size (2–5 μm) that are formed in powders with the lowest and the highest concentration of Ba (BSCF 2882 - **Figure 1a** and BSCF 8282 - **Figure 1e**, respectively). The second category of morphology is represented by particles with round tip branches and with nanoscale features at their surface. Particles with such surface characteristics are observed for the BSCF 4682, BSCF 5582, and BSCF 6482 samples (**Figure 1b–d**). However, these particles are different in size and in shape depending on the Ba content. The powders with the BSCF 4682 (**Figure 1b**) and BSCF 6482 (**Figure 1d**) compositions have particles with dimensions exceeding 10 μm in length, while particles with 50% of Ba are around 3 μm in size (**Figure 1c** – BSCF 5582). Moreover, there are also differences in the shape of these surface microstructures. The particles with BSCF 4682 composition have spherical features on the surface (**Figure 1b**), while for the BSCF 6482 sample (**Figure 1d**) the nanoscale surface structures are elongated and the tendency to agglomerate at the

$Ba_xSr_{1-x}Co_8Fe_2O_{3-\delta}$	Abbreviation	$Ba_{0.5}Sr_{0.5}Co_{1-y}Fe_yO_{3-\delta}$	Abbreviation
$Ba_{0.2}Sr_{0.8}Co_{0.8}Fe_{0.2}O_{3-\delta}$	BSCF 2882	$Ba_{0.5}Sr_{0.5}Co_{0.8}Fe_{0.2}O_{3-\delta}$	BSCF 5582
$Ba_{0.4}Sr_{0.6}Co_{0.8}Fe_{0.2}O_{3-\delta}$	BSCF 4682	$Ba_{0.5}Sr_{0.5}Co_{0.6}Fe_{0.4}O_{3-\delta}$	BSCF 5564
$Ba_{0.5}Sr_{0.5}Co_{0.8}Fe_{0.2}O_{3-\delta}$	BSCF 5582	$Ba_{0.5}Sr_{0.5}Co_{0.4}Fe_{0.6}O_{3-\delta}$	BSCF 5546
$Ba_{0.6}Sr_{0.4}Co_{0.8}Fe_{0.2}O_{3-\delta}$	BSCF 6482	$Ba_{0.5}Sr_{0.5}Co_{0.2}Fe_{0.8}O_{3-\delta}$	BSCF 5528
$Ba_{0.8}Sr_{0.2}Co_{0.8}Fe_{0.2}O_{3-\delta}$	BSCF 8282	$Ba_{0.5}Sr_{0.5}FeO_{3-\delta}$	BSCF 5501

Table 1.
The BSCF compositions analyzed in this study and their corresponding notations.

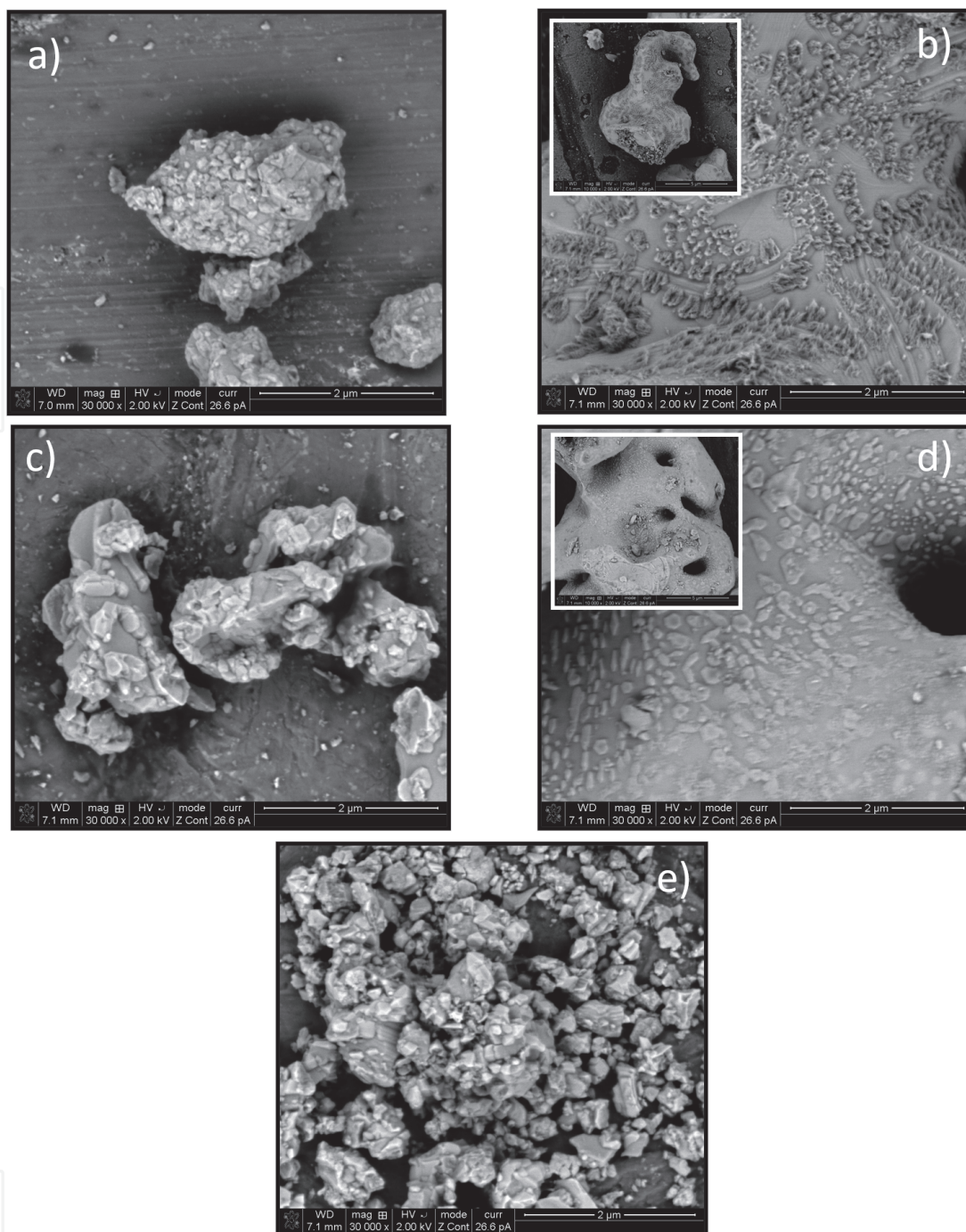


Figure 1.

SEM micrographs of the BSCF powders with increasing Ba content (x): a) BSCF 2882, b) BSCF 4882, c) BSCF 5582, d) BSCF 6482, e) BSCF 8282; scale bar for the main images is 2 μm , while for the inset in b) and d) is 5 μm .

particle tip. The peculiar nanoscaled features on the BSCF particles surface were also observed by other authors for powders prepared by coprecipitation [26] and by solution combustion synthesis [27], and further calcined at temperatures as high as 1273 K. It was claimed that the surface nanostructures induced the high oxygen conductivity of BSCF powders [26]. Another postulated hypothesis is that these nanoscaled features on the surface of BSCF powders appear due to minor amounts of oriented hexagonal phase present as secondary phase [27, 28]. However, BSCF powders prepared by the solid state reaction method used in this study are expected to have a predominantly cubic perovskite structure [20].

The variation of partial molar free energy ($\Delta\bar{G}_{O_2}$) and oxygen partial pressure (p_{O_2}) with temperature is presented in **Figure 2** for the five selected BSCF compositions corresponding to different Ba/Sr ratios with x ranging from 0.2 to 0.8.

The variation of $\Delta\bar{G}_{O_2}$ and $\log p_{O_2}$ with temperature is not monotonous. In the temperature range of 823–923 K, the BSCF 5582 and BSCF 2882 exhibited the highest values of partial molar free energy, while in the domain 923–1223 K, the highest partial molar free energy values were noted for BSCF 6482. For instance, in this temperature range, $\Delta\bar{G}_{O_2}$ value for BSCF 6482 is up to 30 kJ mol⁻¹ higher compared to that of the BSCF 5582 sample. BSCF 5582 exhibited the flattest variation of $\Delta\bar{G}_{O_2}$ with temperature in the entire temperature domain 823–1273 K. The highest oxygen vacancy concentration is expected for the BSCF 6482 composition, as high $\Delta\bar{G}_{O_2}$ values were recorded. A higher oxygen vacancy concentration means more carriers for oxygen transport. Therefore, a higher oxygen ionic conductivity is envisaged for BSCF 6482 above 923 K. This statement is consistent with the electrical conductivity and improved electrochemical performance reported for the BSCF 6482-based cathode material at these temperatures [29]. High oxygen conductivity and oxygen permeability at intermediate temperatures were also reported for the BSCF 5582 composition [16, 30]. Doping with 50–60% Ba stabilizes the lower oxidation states of the B-site cations, holding the perovskite-structure more effectively and thus contributing indirectly to the enhanced electrochemical performance for these compositions [31, 32].

To get insights into the energetics of oxygen vacancy formation, the partial molar enthalpy and entropy of oxygen dissolution in the perovskite lattice ($\Delta\bar{H}_{O_2}$ and $\Delta\bar{S}_{O_2}$, respectively) were calculated in the temperature domains in which the partial molar free energies are linear functions of temperature. For each sample, these particular temperature domains are: 973–1123 K and 1123–1223 K for BSCF 2882; 973–1073 K and 1073–1173 K for BSCF 4682; 973–1073 K and 1073–1223 K for BSCF 5582; 923–1023 K and 1023–1173 K for BSCF 6482; 923–1023 K and 1023–1123 K for BSCF 8282 (**Figure 3a**). The thermodynamic investigation pointed out that the temperature of structural transformations (T_{tr}) decreases as Ba (x) content increases, being 1123 K for $x = 0.2$; 1073 K for $x = 0.4$ and $x = 0.5$; 1023 K for $x = 0.6$ and $x = 0.8$.

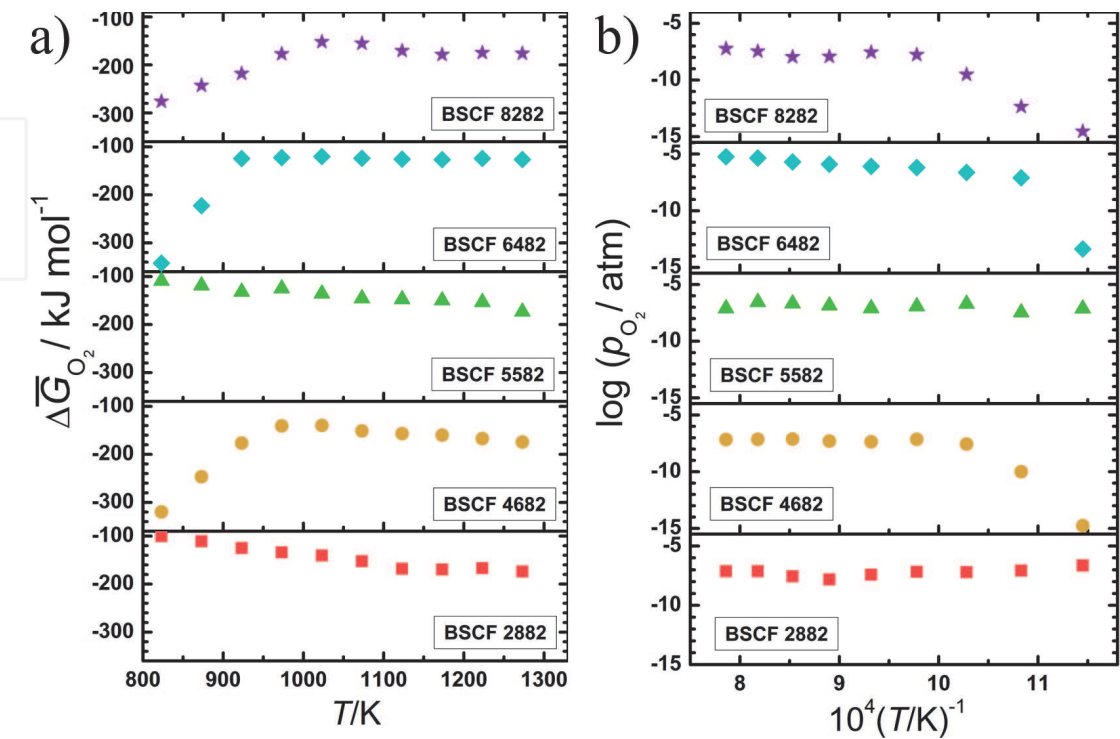


Figure 2.
Variation of a) $\Delta\bar{G}_{O_2}$ and b) $\log p_{O_2}$ with the Temperature and Ba-content (x).

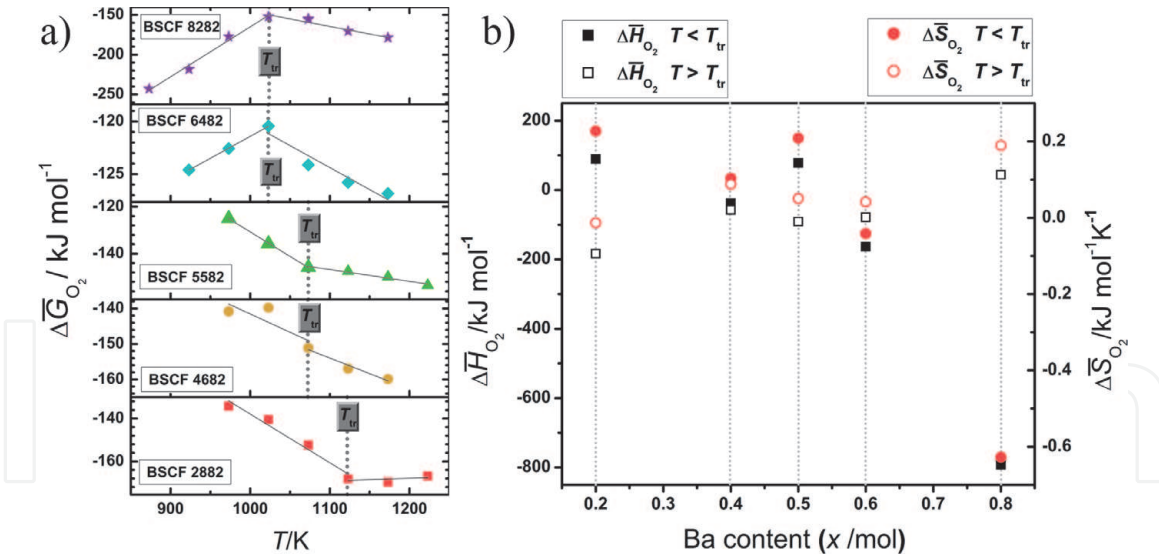


Figure 3.

a) Variation of $\Delta \bar{G}_{O_2}$ with temperature and Ba content (x) - linear fit in the selected temperature domain; b) $\Delta \bar{H}_{O_2}$ and $\Delta \bar{S}_{O_2}$ versus Ba content (x) before and after T_{tr} defined in a).

The variation of $\Delta \bar{H}_{O_2}$ and $\Delta \bar{S}_{O_2}$ with Ba content is depicted in **Figure 3b**. At temperatures lower than T_{tr} , the $\Delta \bar{H}_{O_2}$ and $\Delta \bar{S}_{O_2}$ for the samples with 20, 40 and 50% of Ba are in the similar range. As the Ba concentration increases, the partial molar enthalpy and entropy values drastically decrease, reaching values as low as -792 kJ mol^{-1} and $-627 \text{ J mol}^{-1} \text{K}^{-1}$, respectively, for the BSCF 8282 composition.

This decrease of $\Delta \bar{H}_{O_2}$ and $\Delta \bar{S}_{O_2}$ is associated with an increase of the binding energy of oxygen and an increase of order in the oxygen sublattice of the perovskite-type structure, respectively. At temperatures higher than the points of transitions, both $\Delta \bar{H}_{O_2}$ and $\Delta \bar{S}_{O_2}$ increased as the Ba-content increases. For BSCF 5582 and BSCF 6482 specimens these values are similar. Thus, besides the oxygen vacancy concentration, the ordering of the oxygen vacancy has a remarkable influence on the entropy values being an indication that the oxygen vacancies are distributed randomly on the oxygen sublattice.

In the intermediate temperature range below 1173 K the variations of the thermodynamic data show some anomalies, which could be correlated with the transition to the cubic BSCF structures [32]. These structural transformations are connected to the charge compensation mechanism. Crystal structure and electrical conductivity of several selected compositions in the Ba–Sr–Co–Fe–O system indicate that doping with more Ba into the system increases the ability for lattice oxygen exchange [13, 20, 21, 33]. A reversible phase transition from cubic to mixed phase of cubic and hexagonal at 973–1173 K for the BSCF 5582 compositions was pointed out both experimentally (employing coulometric titrations and thermal analysis [14, 20, 21, 32–35] and theoretically, by applying the density functional theory calculations [36, 37].

Keeping in mind the key role of oxygen vacancy ordering on the crystalline phase formation, the less symmetrical non-cubic phases are expected to have highly ordered oxygen vacancies. When the temperature increases above 1023 K, the vacancy ordering starts to disappear, the oxygen vacancies become more mobile and the crystalline phase of the material tends to exhibit higher symmetry, but lower stability. Both, the thermodynamic data and the phase symmetry results let us conclude that low symmetric BSCF perovskites, like BSCF 5582, BSCF 6482 and BSCF 4682 are thermodynamically more stable than the high symmetric BSCF perovskite.

3.2 B-site effect: Co/Fe variation

The morphological evolution of the as prepared BSCF powders with increasing Fe content, is shown in **Figure 4** for a) $y = 0.2$, b) $y = 0.4$, c) $y = 0.6$, d) $y = 0.8$, and e) $y = 1.0$. Well defined nanoscale features are shown in **Figure 4a** for the BSCF 5582 sample (see also **Figure 1c**). In contrast, smooth surfaces formed on the particles in the BSCF 5546 and the BSCF 5564 compositions (**Figure 4b** and **c**). The BSCF 5528 and the BSCF 5501 powders have a rough surface showing the incipient formation of the nanostructured features on the surface (**Figure 4d** and **e**). It is therefore expected that these samples to contain a very small quantity of the hexagonal secondary phase [27], not detectable by X-ray diffraction [20].

In **Figure 5**, the variation with temperature of the partial molar free energy (a) and of the oxygen partial pressure (b) is shown for the BSCF compositions with variable Fe content ($0.2 \leq y \leq 1$).

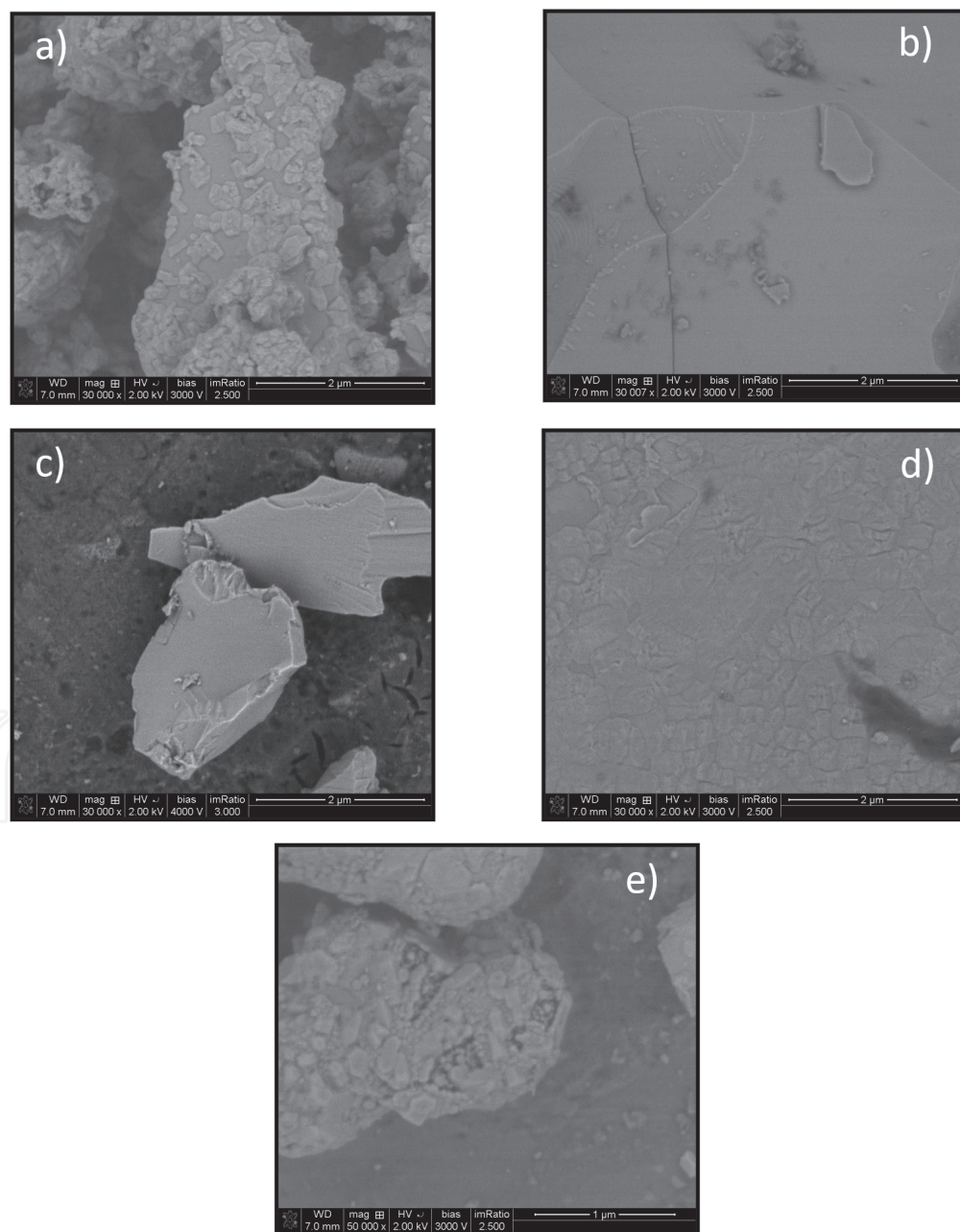


Figure 4.
 SEM micrographs of the BSCF powders with increasing Fe content (y): a) BSCF 5582, b) BSCF 5564, c) BSCF 5546, d) BSCF 5528, e) BSCF 5501; scale bar for the images is $2 \mu\text{m}$, except for e) where it is $1 \mu\text{m}$.

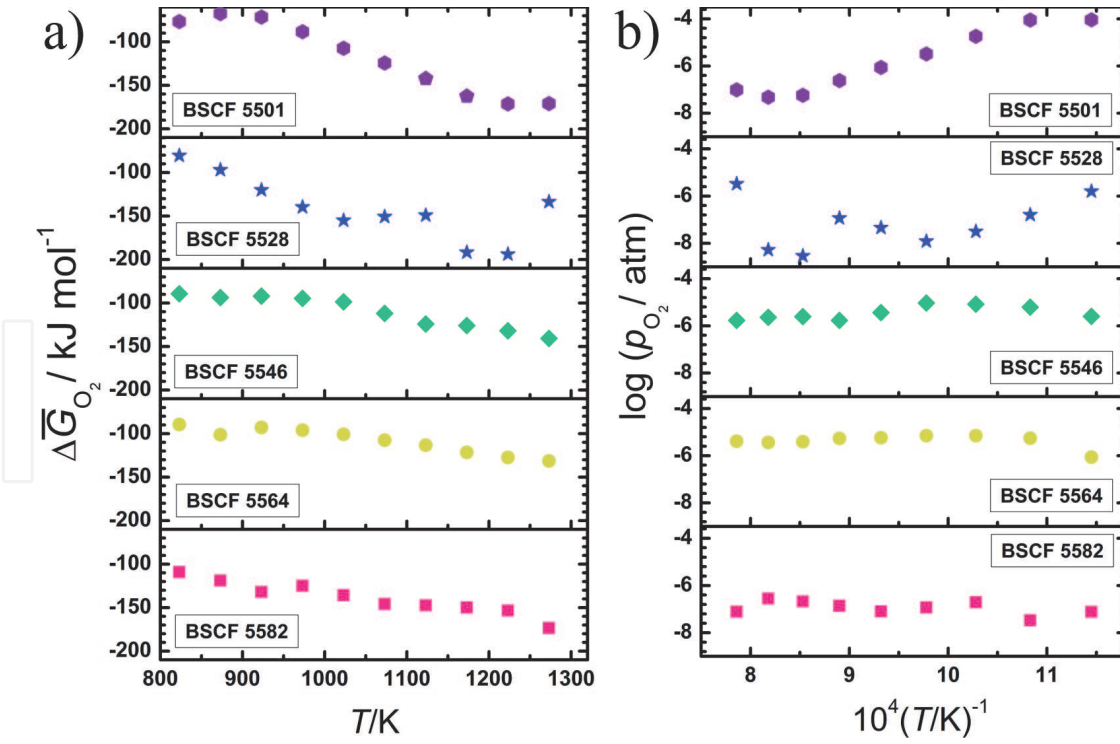


Figure 5.
a) $\Delta\bar{G}_{O_2}$ and b) $\log p_{O_2}$ with the temperature and Fe content (y).

The heated samples exhibited a complex behavior in the entire investigated temperature domain. One can observe that, in the intermediate temperature range from 823 K to 973 K, the BSCF 5501 sample has the highest recorded values for both $\Delta\bar{G}_{O_2}$ and $\log p_{O_2}$, while, in the high temperature range from 1073 K to 1273 K, the highest values were obtained for the BSCF 5564 composition. This suggests the highest concentration of oxygen vacancies in the specified temperature ranges for these samples. The results could be correlated to the high oxygen non-stoichiometry [1], high ionic conductivity [38], as well as with the lattice expansion (volume effect) of the crystalline structure [39] reported for these compositions. For the BSCF 5582 it has been reported that about 60% of the Co^{3+} ions are oxidized to Co^{4+} ($r_{Co^{4+}} = 0.67 \text{ \AA}$), while, at the same time, all the Fe^{3+} ions are into high valence state (Fe^{4+} with $r_{Fe^{4+}} = 0.73 \text{ \AA}$), thus this effect has to be compensated by oxygen vacancy formation [40, 41]. Increasing iron content in the heat-treated samples at 1173 K and 1223 K, the decrease of the non-stoichiometry and of the total electrical conductivity is expected [1, 40]. This effect was also evidenced for various substituted ABO_3 perovskites solid solution series (e.g. $La_{1-x}Sr_xCo_{1-y}Fe_yO_{3-\delta}$ [42, 43] and $La_{1-x}Sr_xMn_{1-y}Fe_yO_{3-\delta}$ [44]) where the formation of oxygen vacancies decreased with Fe content.

The values for the partial molar enthalpy and entropy, $\Delta\bar{H}_{O_2}$ and $\Delta\bar{S}_{O_2}$, respectively, were calculated in the temperature ranges in which the partial molar free energies are linear functions of temperature (**Figure 5a**). These specific temperature domains are 973–1073 K and 1073–1223 K for BSCF 5582; 973–1273 K for BSCF 5564; 923–1023 K and 1023–1123 K for BSCF 5546 and 923–1173 K for BSCF 5501. The temperatures of transition (T_{tr}) were established at: 1073 K for $y = 0.2$, 1023 K for $y = 0.6$ and 1023 K for $x = 0.8$. The variation of $\Delta\bar{H}_{O_2}$ and $\Delta\bar{S}_{O_2}$ with Fe content, below and above T_{tr} , are depicted in **Figure 6b**. At temperatures below the transition temperature, $\Delta\bar{H}_{O_2}$ and $\Delta\bar{S}_{O_2}$ values of the BSCF compositions having 20, 40 and 60% Fe slightly decreased, and then increased again for the 80 and 100% of Fe concentrations. Our results correlate well with the parabolic variation in ionic

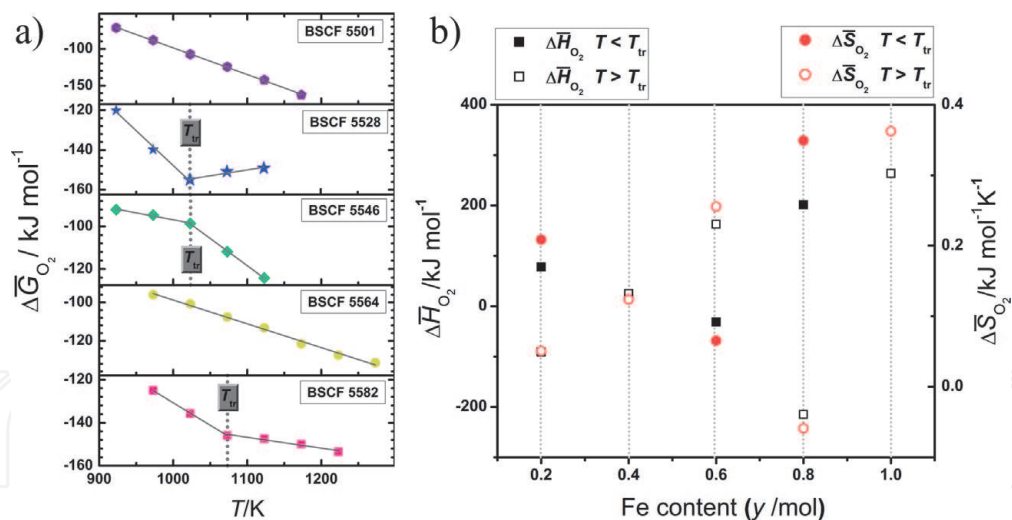


Figure 6.

a) Partial molar enthalpy $\Delta\bar{G}_{\text{O}_2}$ with temperature and Fe content (y) - linear fit in the selected temperature domains; b) partial molar enthalpy and entropy $\Delta\bar{H}_{\text{O}_2}$ and $\Delta\bar{S}_{\text{O}_2}$ as a function of Fe content (y) before and after T_{tr} defined in a).

conductivity *versus* iron content (with the identification of a minimum ionic conductivity at around 50% Fe-content) noted for $\text{Ba}_{1-x}\text{Sr}_x\text{Co}_{1-y}\text{Fe}_y\text{O}_{2.5}$ system [45]. This behavior is ascribed to the largest amount of oxygen vacancy trapped around Sr and Co ions for the composition containing $\sim 50\%$ iron. Above the T_{tr} , both $\Delta\bar{H}_{\text{O}_2}$ and $\Delta\bar{S}_{\text{O}_2}$ increased with the Fe-content increasing, except the values obtained for BSCF 5528. The increase of the partial molar enthalpy and entropy values with Fe content follows the order: BSCF 5582 < BSCF 5564 < BSCF 5546 < BSCF 5501 and suggests the decrease of the binding energy of oxygen in the lattice and a random distribution of the oxygen vacancies in the oxygen sublattice of the perovskite-type structure with the iron content. This mean that the thermodynamic stability of $\text{Ba}_{0.5}\text{Sr}_{0.5}\text{Co}_{1-y}\text{Fe}_y\text{O}_{3-\delta}$ increased in the following order $y = 1 < y = 0.6 < y = 0.4 < y = 0.2$, the specimen BSCF 5582 being the most stable composition for temperature $\geq 1023 \text{ K}$. This finding can be explained by the relative redox stability of the B^{3+} ions which seems to modify both the mobility and the concentration of the oxygen vacancies, at the same A-site composition. Moreover, the substitution of Co by Fe induces a stabilization of cubic perovskite structure [20, 46].

The BSCF 5528 sample has a distinct thermodynamic behavior which is further discussed. At temperatures lower than 1023 K , the values of enthalpy and entropy of 264 kJ mol^{-1} and $362 \text{ J mol}^{-1}\text{K}^{-1}$, respectively were obtained (**Figure 6b**). In the interval $1023\text{--}1123 \text{ K}$ a strong decrease of the partial molar enthalpy and entropy was observed to values as low as -215 kJ mol^{-1} and $-58.9 \text{ J mol}^{-1}\text{K}^{-1}$, respectively. In this temperature domain the BSCF 5528 sample exhibits high thermodynamic stability. Between 1173 and 1223 K , the variation of the partial molar free energy is observed (**Figure 5a**), which can be due to further structural transformation related to the charge compensation mechanism. The result is in accordance with the literature indicating the presence of secondary phases in the X-ray diffraction patterns of the samples following the thermal cycle at 1173 K [39]. At the same time, a sharp decrease in the permeation flux was reported for BSCF membranes with the increase of iron concentration from 60 to 80% [1]. The results suggest that the increase of iron concentration in BSCF might be hindered more by the slow oxygen bulk diffusion than by the surface exchange kinetics of the oxides. This could also explain the behavior of the BSCF 5528 sample at 1273 K for which the partial molar free energy increases with $\sim 40 \text{ kJ mol}^{-1}$ above the values corresponding to all the other investigated samples.

3.3 Oxygen non-stoichiometry effect

In order to further evaluate the previous results, the influence of the change of the oxygen stoichiometry on the thermodynamic properties was examined by solid state coulometric titration technique coupled with EMF measurements. The oxygen stoichiometry was modified by decreasing the stoichiometry with the same relative deviation of $\Delta\delta = 0.01$ for all the BSCF compositions. Further, the effect of the oxygen non-stoichiometry was correlated with the influence of the A- and B-site dopant.

Two sets of data representing the $\Delta\bar{G}_{O_2}$ change before and after the isothermal titration experiments, in the temperature range 1123–1273 K, for BSCF compositions are plotted in **Figure 7(a)** (for the samples with Ba-content increasing) and **Figure 7(b)** (for the samples with variable Fe concentration).

After titration, the decrease of $\Delta\bar{G}_{O_2}$ values with the stoichiometry change is observed for all the investigated compositions with various Ba- and Fe-dopant concentrations, except for the sample BSCF 5528 containing 80% Fe. The obtained results suggested that the energy of vacancy formation decreases with increasing non-stoichiometry while for BSCF 5528 an opposite behavior is estimated.

Considering the partial pressure of oxygen as a key parameter for the thermodynamic characterization of the materials, the variation of the $\log p_{O_2}$ with the temperature and the concentration of the dopants at the same deviation from stoichiometry was analyzed. The results are presented in **Figure 8**.

A decrease of $\log p_{O_2}$ with the relative non-stoichiometry change (δ) is observed for both series of BSCF compositions enriched in Ba (**Figure 8a**) and Fe (**Figure 8b**), excepting BSCF 5528 specimen. The obtained results for the BSCF analyzed compositions confirmed that at temperatures from 1123 K to 1273 K, the oxygen vacancies are generated at the expense of electron holes. The charge imbalance caused by the B-site substitution starts to be compensated by the formation of the oxygen vacancies. After oxygen coulometric titration, the highest deviation in the $\log p_{O_2}$ values with the stoichiometry is obtained for the sample containing 100% of Fe (BSCF 5501). This, in turn, is accompanied by the highest decrease in the concentration of oxygen vacancies comparing to the other compositions.

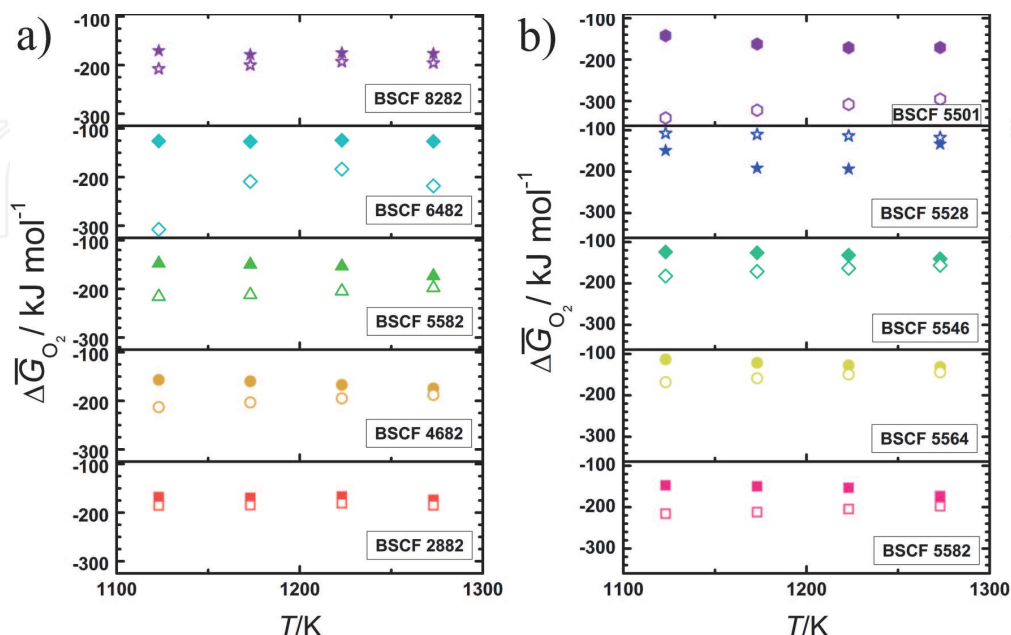


Figure 7.

$\Delta\bar{G}_{O_2}$ vs. temperature for BSCF compounds with a) Ba-content (x) and b) Fe-content (y) variance showing the effect of the oxygen non-stoichiometry; solid symbols in each graph represent the values recorded before titration, while empty symbols indicate the corresponding values after titration.

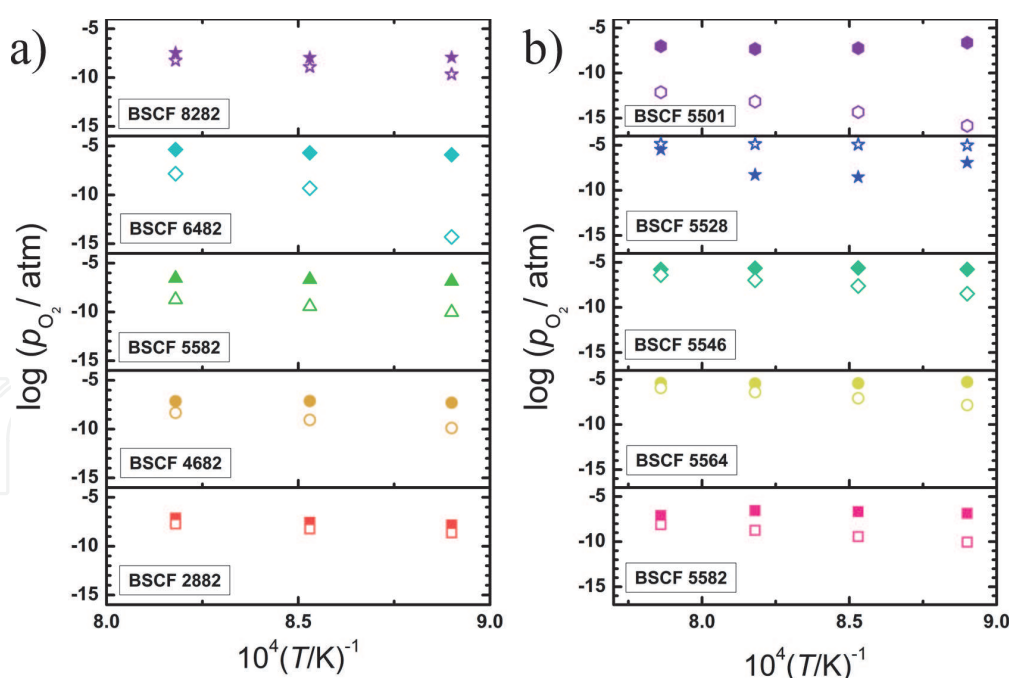


Figure 8. Variation of $\log p_{O_2}$ with temperature for BSCF compounds with a) Ba-content (x) and b) Fe-content (y) variance showing the effect of the oxygen non-stoichiometry; solid symbols in each graph represent the values recorded before titration, while empty symbols indicate the corresponding values after titration.

The changes of $\Delta\bar{H}_{O_2}$ and $\Delta\bar{S}_{O_2}$ with the oxygen non-stoichiometry were evaluated for the BSCF compositions (**Figure 9**). For BSCF 6482 and BSCF 5528, the values of enthalpy and entropy were not included in **Figure 9a** and **9b**, respectively due to the deviation from linearity of the energy values obtained in the temperature domain 1123–1273 K. For both BSCF series with Ba- and Fe- compositional variations, the values of enthalpies and entropies decreased with stoichiometry change suggesting an increase in the binding energy of oxygen and change of order in the oxygen sublattice of the perovskite-type structure.

The $\Delta\bar{H}_{O_2}$ and $\Delta\bar{S}_{O_2}$ did not indicate a clear tendency of variation with barium concentration at the same deviation of stoichiometry, our results being consistent with the results of Girdauskaite *et al.* [47].

For the BSCF series with different Fe-content, a strong decrease of partial molar enthalpy with δ and with increasing of Fe-content was recorded, particularly for the sample with the highest Fe content. This result along with the negative enthalpy values indicated that the thermodynamic stability increased in the following order BSCF 5582 < BSCF 5564 < BSCF 5546 < BSCF 5501. Regarding the entropy, an abrupt decrease for the samples containing 20, 40 and 60% iron was observed, while for the composition containing only Fe in B-site, a slight $\Delta\bar{S}_{O_2}$ diminution with δ was noticed. The values of partial entropies of oxygen dissolution for $y = 0.2, 0.4$, and 0.6 are negative, which is an indicative for a metal vacancy mechanism [48, 49]. Due to the large decrease in $\Delta\bar{S}_{O_2}$ for the samples with $y = 0.2; 0.4$ and 0.6 , it is considered that the oxygen vacancies would not randomly distribute on all of the oxygen sites but they would be distributed to some particular oxygen sites. This means that the total number of sites employed by oxygen vacancies is decreased. It is also possible that the vacancy distribution is related to some crystallographic distortions or ordering of metal sites. The result is in agreement with previous reports noting the formation of partially ordered oxygen vacancies in highly defective perovskite-type oxides [42, 50, 51].

The thermodynamic data showed that, after titration, BSCF 5501 is the most stable composition, exhibiting an increased binding energy of oxygen in the lattice but a

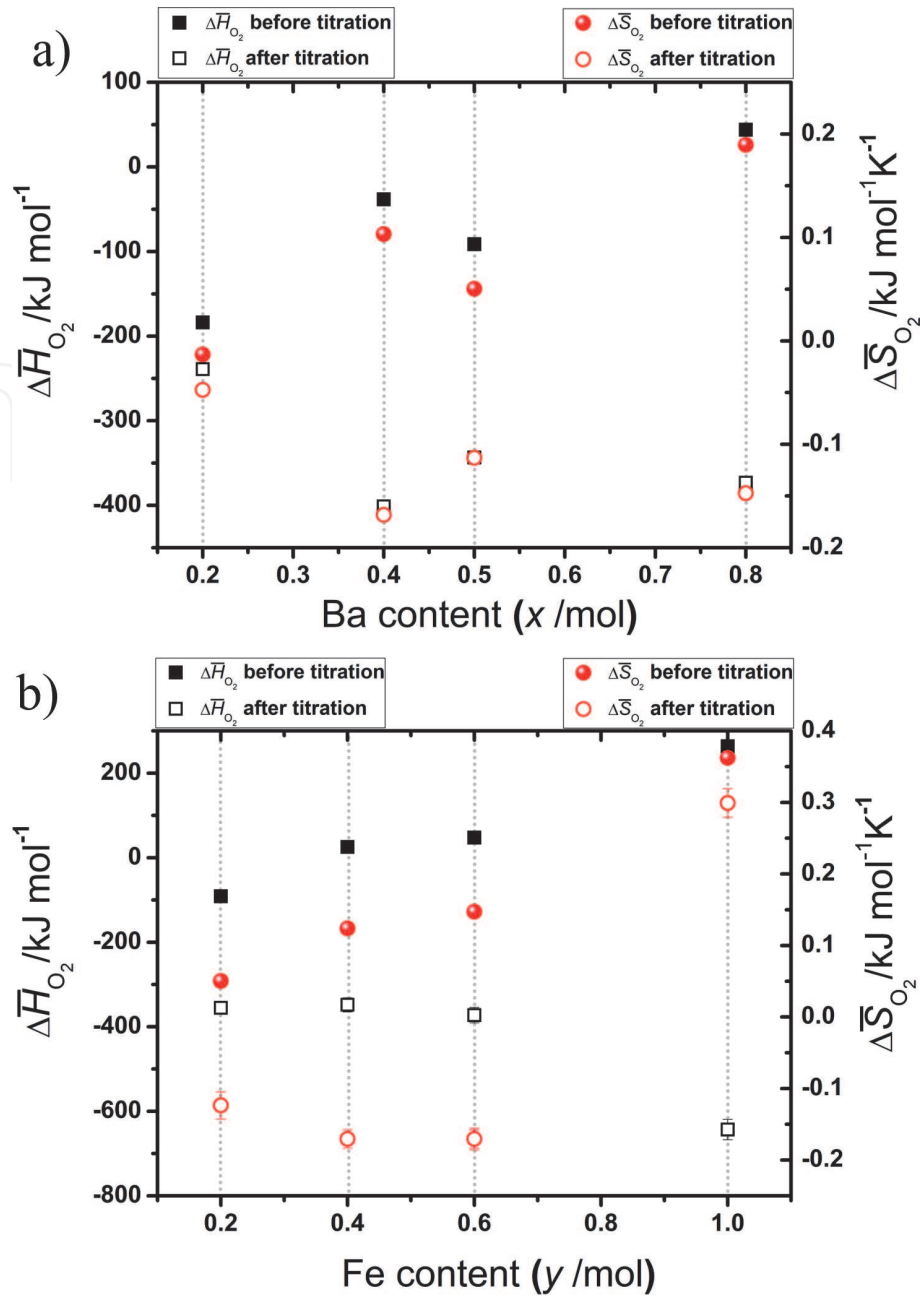


Figure 9.

ΔH_{O_2} and ΔS_{O_2} as a function of a) Ba and b) Fe content and illustrating the effect of the oxygen non-stoichiometry at temperatures above 1123 K.

random distribution of oxygen vacancies within the oxygen sublattice. The result is consistent with the morphological investigation as well as with the high stability of cubic perovskite phase evaluated for Sr- and Fe- rich compositions [20, 46].

The thermodynamics of solid solutions containing a mixture of cobalt and iron on the B-site is complex. Further details and measurements of the energy and the entropy of oxygen incorporation into BSCF at different values of non-stoichiometry δ are necessary in order to make clear the effect of the stoichiometry change on the vacancy distribution within the oxygen sublattice.

4. Conclusions

The thermodynamic behavior of BSCF compounds with different Ba and Fe contents, using an electrochemical cell with yttria-stabilized zirconia as solid electrolyte was investigated. The EMF measurements performed in a wide temperature

range (823–1273 K) and at pressures of 10^{-5} – 10^{-6} Pa confirm the instability of the BSCF-perovskite phases at temperatures lower than 1123 K.

With the help of the thermodynamic data, the points of phase transformations associated with the charge compensation mechanism were highlighted, the results being important for the assessment of the long-term stability of such nonstoichiometric materials used as cathodes in IT-SOFCs. The temperature associated to the structural transformations decreases with the increase of Ba-content. The thermodynamic investigation evidenced that for the system $Ba_xSr_{1-x}Co_{0.8}Fe_{0.2}O_{3-\delta}$, low symmetry BSCF-perovskites (BSCF 5582, BSCF 6482 and BSCF 4682) are thermodynamically more stable than high symmetry BSCF-perovskites (BSCF 2882 and BSCF 8282). In the case of $Ba_{0.5}Sr_{0.5}Co_{1-y}Fe_yO_{3-\delta}$ with different iron-content, at temperatures ≥ 1023 K, thermodynamic stability increased following the order $y = 1 < y = 0.6 < y = 0.4 < y = 0.2$, the composition BSCF 5582 being the most stable in the series, while the composition with $y = 0.8$ exhibited a peculiar behavior.

The BSCF compounds exhibited a significant variation of the thermodynamic parameters with the oxygen non-stoichiometry change, this variation being highly dependent on temperature and dopant concentration. The thermodynamic data evidenced that after decreasing the oxygen stoichiometry with the same relative deviation of $\Delta\delta = 0.01$, the specimen BSCF 5501 was the most stable composition within 1123–1273 K temperature range. The results of the thermodynamic study of BSCF compounds, at temperatures of interest for the application in IT-SOFC help us to explain why the BSCF 5582 composition exhibits the highest ionic conductivity and the highest oxygen catalytic activity.

Knowing the specific thermodynamic quantities of BSCF compositions, it is possible to find new routes to modify the properties of these materials by suitable substitution and formation of oxygen vacancies in oxygen lattice. The evaluation of thermodynamic quantities is mandatory to understand the complex relationships between the defect chemistry and the material properties.

Author details


Florentina Maxim¹, Alina Botea-Petcu¹, Florina Teodorescu^{1*}, Ludwig J. Gauckler² and Speranta Tanasescu¹

¹ “Ilie Murgulescu” Institute of Physical Chemistry of the Romanian Academy, Laboratory of Chemical Thermodynamics, Bucharest, Romania

² Nonmetallic Inorganic Materials, Department of Materials, ETH Zürich, Zürich, Switzerland

*Address all correspondence to: fteodorescu@icf.ro

IntechOpen

© 2020 The Author(s). Licensee IntechOpen. This chapter is distributed under the terms of the Creative Commons Attribution License (<http://creativecommons.org/licenses/by/3.0>), which permits unrestricted use, distribution, and reproduction in any medium, provided the original work is properly cited. 

References

- [1] Chen ZH, Ran R, Zhou W, Shao ZP, Liu SM. Assessment of $\text{Ba}_{0.5}\text{Sr}_{0.5}\text{Co}_{1-y}\text{Fe}_y\text{O}_{3-\delta}$ ($y=0.0-1.0$) for prospective application as cathode for IT-SOFCs or oxygen permeating membrane. *Electrochim Acta*. 2007;52(25):7343–51. DOI: 10.1016/j.electacta.2007.06.010
- [2] McIntosh S, Vente J, Haije W, Blank D, Bouwmeester H. Structure and oxygen stoichiometry of $\text{SrCo}_{0.8}\text{Fe}_{0.2}\text{O}_{3-\delta}$ and $\text{Ba}_{0.5}\text{Sr}_{0.5}\text{Co}_{0.8}\text{Fe}_{0.2}\text{O}_{3-\delta}$. *Solid State Ionics*. 2006;177(19–25):1737–42. DOI: 10.1016/j.ssi.2006.03.041
- [3] McIntosh S, Vente JF, Haije WG, Blank DHA, Bouwmeester HJM. Oxygen stoichiometry and chemical expansion of $\text{Ba}_{0.5}\text{Sr}_{0.5}\text{Co}_{0.8}\text{Fe}_{0.2}\text{O}_{3-\delta}$ measured by *in situ* neutron diffraction. *Chem Mater*. 2006;18(8):2187–93. DOI: 10.1021/cm052763x
- [4] Vente JF, McIntosh S, Haije WG, Bouwmeester HJM. Properties and performance of $\text{Ba}_x\text{Sr}_{1-x}\text{Co}_{0.8}\text{Fe}_{0.2}\text{O}_{3-\delta}$ materials for oxygen transport membranes. *J Solid State Electr*. 2006;10(8):581–8. DOI: 10.1007/s10008-006-0130-2
- [5] Bucher E, Egger A, Ried P, Sitte W, Holtappels P. Oxygen nonstoichiometry and exchange kinetics of $\text{Ba}_{0.5}\text{Sr}_{0.5}\text{Co}_{0.8}\text{Fe}_{0.2}\text{O}_{3-\delta}$. *Solid State Ionics*. 2008;179(21–26):1032–5. DOI: 10.1016/j.ssi.2008.01.089
- [6] Sadykov VA, Sadovskaya EM, Uvarov NF. Methods of isotopic relaxations for estimation of oxygen diffusion coefficients in solid electrolytes and materials with mixed ionic-electronic conductivity. *Russ. J. Electrochem*. 2015;51(5):458–67. DOI: 10.1134/S1023193515050109
- [7] Jung J-I, Mixture ST, Edwards DD. The electronic conductivity of $\text{Ba}_{0.5}\text{Sr}_{0.5}\text{Co}_x\text{Fe}_{1-x}\text{O}_{3-\delta}$ (BSCF: $x=0\sim 1.0$) under different oxygen partial pressures. *J Electroceram*. 2009;24(4):261–9. DOI: 10.1007/s10832-009-9567-x
- [8] Shao Z, Haile SM. A high-performance cathode for the next generation of solid-oxide fuel cells. *Materials for Sustainable Energy*. p. 255–8. DOI: 10.1038/nature02863
- [9] Sahini MG, Tolchard JR, Wiik K, Grande T. High temperature X-ray diffraction and thermo-gravimetric analysis of the cubic perovskite $\text{Ba}_{0.5}\text{Sr}_{0.5}\text{Co}_{0.8}\text{Fe}_{0.2}\text{O}_{3-\delta}$ under different atmospheres. *Dalton T*. 2015;44(23):10875–81. DOI: 10.1039/C4DT03963G
- [10] Waindich A, Möbius A, Müller M. Corrosion of $\text{Ba}_{1-x}\text{Sr}_x\text{Co}_{1-y}\text{Fe}_y\text{O}_{3-\delta}$ and $\text{La}_{0.3}\text{Ba}_{0.7}\text{Co}_{0.2}\text{Fe}_{0.8}\text{O}_{3-\delta}$ materials for oxygen separating membranes under Oxycoal conditions. *J Membrane Sci*. 2009;337(1):182–7. DOI: 10.1016/j.memsci.2009.03.041
- [11] Yáng Z, Harvey AS, Gauckler LJ. Influence of CO_2 on $\text{Ba}_{0.2}\text{Sr}_{0.8}\text{Co}_{0.8}\text{Fe}_{0.2}\text{O}_{3-\delta}$ at elevated temperatures. *Scripta Mater*. 2009;61(11):1083–6. DOI: 10.1016/j.scriptamat.2009.08.039
- [12] Saša Z, Toni I, Sebastien V, Dijana J, J. GL. The changes of $\text{Ba}_{0.5}\text{Sr}_{0.5}\text{Co}_{0.8}\text{Fe}_{0.2}\text{O}_{3-\delta}$ perovskite oxide on heating in oxygen and carbon dioxide atmospheres. *J Serb Chem Soc*. 2014;79(9):13. DOI: 10.2298/JSC131024018Z
- [13] Tanasescu S, Yang Z, Martynczuk J, Varazashvili V, Maxim F, Teodorescu F, Botea A, Totir N, Gauckler LJ. Effects of A-site composition and oxygen nonstoichiometry on the thermodynamic stability of compounds in the Ba-Sr-Co-Fe-O system. *J Solid State Chem*. 2013;200:354–62. DOI: 10.1016/j.jssc.2013.01.030
- [14] Wang F, Nakamura T, Yashiro K, Mizusaki J, Amezawa K. The crystal

structure, oxygen nonstoichiometry and chemical stability of $Ba_{0.5}Sr_{0.5}Co_{0.8}Fe_{0.2}O_{3-\delta}$ (BSCF). *Phys Chem Chem Phys*. 2014;16(16):7307–14. DOI: 10.1039/C3CP54810D

[15] Wang HH, Tablet S, Yang WS, Caro R. *In situ* high temperature X-ray diffraction studies of mixed ionic and electronic conducting perovskite-type membranes. *Mater Lett*. 2005;59(28):3750–5. DOI: 10.1016/j.matlet.2005.06.067

[16] Zhou W, Ran R, Shao Z. Progress in understanding and development of $Ba_{0.5}Sr_{0.5}Co_{0.8}Fe_{0.2}O_{3-\delta}$ -based cathodes for intermediate-temperature solid-oxide fuel cells: A review. *J Power Sources*. 2009;192(2):231–46. DOI: 10.1016/j.jpowsour.2009.02.069

[17] Ovenstone J, Jung JI, White JS, Edwards DD, Misture ST. Phase stability of BSCF in low oxygen partial pressures. *J Solid State Chem*. 2008;181(3):576–86. DOI: 10.1016/j.jssc.2008.01.010

[18] Jung JI, Misture ST, Edwards DD. Seebeck coefficient and electrical conductivity of BSCF ($Ba_{0.5}Sr_{0.5}Co_xFe_{1-x}O_{3-\delta}$, $0 \leq x \leq 0.8$) as a function of temperature and partial oxygen pressure. *Solid State Ionics*. 2012;206:50–6. DOI: 10.1016/j.ssi.2011.09.023

[19] Mueller DN, De Souza RA, Yoo H-I, Martin M. Phase stability and oxygen nonstoichiometry of highly oxygen-deficient perovskite-type oxides: A case study of $(Ba,Sr)(Co,Fe)O_{3-\delta}$. *Chem Mater*. 2012;24(2):269–74. DOI: 10.1021/cm2033004

[20] Yang Z, Harvey AS, Infortuna A, Gauckler LJ. Phase relations in the Ba-Sr-Co-Fe-O system at 1273 K in air. *J Appl Crystallogr*. 2009;42:153–60. DOI: 10.1107/S0021889809002040

[21] Yang Z, Harvey AS, Infortuna A, Schoonman J, Gauckler LJ. Electrical conductivity and defect chemistry of

$Ba_xSr_{1-x}Co_yFe_{1-y}O_{3-\delta}$ perovskites. *J Solid State Electr*. 2011;15(2):277–84. DOI: 10.1007/s10008-010-1208-4

[22] Frank L, Hovorka M, Mikmeková Š, Mikmeková E, Müllerová I, Pokorná Z. Scanning electron microscopy with samples in an electric field. *Materials*. 2012;5(12):2731–56. DOI: 10.3390/ma5122731

[23] Tanasescu S, Totir ND, Marchidan DI. Thermodynamic data of the perovskite-type $LaMnO_{3\pm x}$ and $La_{0.7}Sr_{0.3}MnO_{3\pm x}$ by a solid-state electrochemical technique. *Electrochim Acta*. 1998;43(12–13):1675–81. DOI: 10.1016/S0013-4686(97)00311-3

[24] Tanasescu S, Totir ND, Marchidan DI, Turcanu A. The influence of compositional variables on the thermodynamic properties of lanthanum strontium ferrite manganites and lanthanum strontium manganites. *Mater Res Bull*. 1997;32(7):915–23. DOI: 10.1016/S0025-5408(97)00054-8

[25] Tanasescu S, Totir ND, Marchidan DI. Thermodynamic properties of the $SrFeO_{2.5}$ and $SrMnO_{2.5}$ brownmillerite-like compounds by means of EMF-measurements. *Solid State Ionics*. 2000;134(3–4):265–70. DOI: 10.1016/S0167-2738(00)00731-1

[26] Toprak MS, Darab M, Syvertsen GE, Muhammed M. Synthesis of nanostructured BSCF by oxalate co-precipitation – As potential cathode material for solid oxide fuels cells. *Int J Hydrogen Energ*. 2010;35(17):9448–54. DOI: 10.1016/j.ijhydene.2010.03.121

[27] Deganello F, Liotta L, Marci G, Fabbri E, Traversa E. Strontium and iron-doped barium cobaltite prepared by solution combustion synthesis: exploring a mixed-fuel approach for tailored intermediate temperature solid oxide fuel cell cathode materials. *Mater Renew Sustain Energy*. 2013;2(1):1–14. DOI: 10.1007/s40243-013-0008-z

- [28] Giuliano A, Carpanese MP, Clematis D, Boaro M, Pappacena A, Deganello F, et al. Infiltration, Overpotential and Ageing Effects on Cathodes for Solid Oxide Fuel Cells: $\text{La}_{0.6}\text{Sr}_{0.4}\text{Co}_{0.2}\text{Fe}_{0.8}\text{O}_{3-\delta}$ versus $\text{Ba}_{0.5}\text{Sr}_{0.5}\text{Co}_{0.8}\text{Fe}_{0.2}\text{O}_{3-\delta}$. *J Electrochem Soc.* 2017;164(10):F3114-F22. DOI: : 10.1149/2.0161710jes
- [29] Zhao HL, Shen W, Zhu ZM, Li X, Wang ZF. Preparation and properties of $\text{Ba}_x\text{Sr}_{1-x}\text{Co}_y\text{Fe}_{1-y}\text{O}_{3-\delta}$ cathode material for intermediate temperature solid oxide fuel cells. *J Power Sources.* 2008; 182(2):503–9. DOI: 10.1016/j.jpowsour.2008.04.046
- [30] Berenov A, Atkinson A, Kilner J, Ananyev M, Eremin V, Porotnikova N, et al. Oxygen tracer diffusion and surface exchange kinetics in $\text{Ba}_{0.5}\text{Sr}_{0.5}\text{Co}_{0.8}\text{Fe}_{0.2}\text{O}_{3-\delta}$. *Solid State Ionics.* 2014;268:102–9. DOI: 10.1016/j.ssi.2014.09.031
- [31] Jung J-I, Jeong HY, Kim MG, Nam G, Park J, Cho J. Fabrication of $\text{Ba}_{0.5}\text{Sr}_{0.5}\text{Co}_{0.8}\text{Fe}_{0.2}\text{O}_{3-\delta}$ Catalysts with Enhanced Electrochemical Performance by Removing an Inherent Heterogeneous Surface Film Layer. *Adv Mater.* 2015;27(2):266–71. DOI: 10.1002/adma.201403897
- [32] Müller P, Stormer H, Dieterle L, Niedrig C, Ivers-Tiffée E, Gerthsen D. Decomposition pathway of cubic $\text{Ba}_{0.5}\text{Sr}_{0.5}\text{Co}_{0.8}\text{Fe}_{0.2}\text{O}_{3-\delta}$ between 700 and 1000 °C analyzed by electron microscopic techniques. *Solid State Ionics.* 2012;206:57–66. DOI: 10.1016/j.ssi.2011.10.013
- [33] Yang Z, Martynczuk J, Efimov K, Harvey AS, Infortuna A, Kocher P, et al. Oxygen-vacancy-related structural phase transition of $\text{Ba}_{0.8}\text{Sr}_{0.2}\text{Co}_{0.8}\text{Fe}_{0.2}\text{O}_{3-\delta}$. *Chem Mater.* 2011;23(13):3169–75. DOI: 10.1021/cm200373r
- [34] Efimov K, Xu Q, Feldhoff A. Transmission electron microscopy study of $\text{Ba}_{0.5}\text{Sr}_{0.5}\text{Co}_{0.8}\text{Fe}_{0.2}\text{O}_{3-\delta}$ perovskite decomposition at intermediate temperatures. *Chem Mater.* 2010;22(21):5866–75. DOI: 10.1021/cm101745v
- [35] Harvey AS, Litterst FJ, Yang Z, Rupp JLM, Infortuna A, Gauckler LJ. Oxidation states of Co and Fe in $\text{Ba}_{1-x}\text{Sr}_x\text{Co}_{1-y}\text{Fe}_y\text{O}_{3-\delta}$ ($x, y=0.2-0.8$) and oxygen desorption in the temperature range 300–1273 K. *Phys Chem Chem Phys.* 2009;11(17):3090–8. DOI: 10.1039/B819414A
- [36] Kuklja MM, Mastrikov YA, Jansang B, Kotomin EA. First principles calculations of $(\text{Ba},\text{Sr})(\text{Co},\text{Fe})\text{O}_{3-\delta}$ structural stability. *Solid State Ionics.* 2013;230:21–6. DOI: 10.1016/j.ssi.2012.08.022
- [37] Merkle R, Mastrikov YA, Kotomin EA, Kuklja MM, Maier J. First principles calculations of oxygen vacancy formation and migration in $\text{Ba}_{1-x}\text{Sr}_x\text{Co}_{1-y}\text{Fe}_y\text{O}_{3-\delta}$ perovskites. *J Electrochem Soc.* 2012;159(2):B219-B26. DOI: 10.1149/2.077202jes
- [38] Jung J-I, Misture ST, Edwards DD. Oxygen stoichiometry, electrical conductivity, and thermopower measurements of BSCF ($\text{Ba}_{0.5}\text{Sr}_{0.5}\text{Co}_x\text{Fe}_{1-x}\text{O}_{3-\delta}$, $0 \leq x \leq 0.8$) in air. *Solid State Ionics.* 2010;181(27–28): 1287–93. DOI: 10.1016/j.ssi.2010.06.033
- [39] Magnone E, Miyayama M, Traversa E. Structural properties and electrochemical characteristics of $\text{Ba}_{0.5}\text{Sr}_{0.5}\text{Co}_{1-x}\text{Fe}_x\text{O}_{3-\delta}$ phases in different atmospheres. *J Electrochem Soc.* 2009;156(9):B1059-B66. DOI: 10.1149/1.3158745
- [40] Magnone E, Miyayama M, Traversa E. Some structural considerations on the perovskite-type $\text{A}_{1-y}\text{Sr}_y\text{Co}_{1-x}\text{Fe}_x\text{O}_{3-\delta}$ solid solution series. *Cryst Res Technol.* 2010;45(4):355–64. DOI: 10.1002/crat.200900704
- [41] Celorrio V, Tiwari D, Fermin DJ. Composition-dependent reactivity of $\text{Ba}_{0.5}\text{Sr}_{0.5}\text{Co}_x\text{Fe}_{1-x}\text{O}_{3-\delta}$ toward the

Oxygen Reduction Reaction. J Phys Chem C. 2016;120(39):22291–7. DOI: 10.1021/acs.jpcc.6b04781

properties of $Ln_{0.5}Sr_{0.5}FeO_3$ (Ln: La, Pr). J Saudi Chem Soc. 2012;16(1):91–5. DOI: 10.1016/j.jscs.2010.11.004

[42] Lankhorst MHR, Bouwmeester HJM, Verweij H. High-temperature coulometric titration of $La_{1-x}Sr_xCoO_{3-\delta}$: Evidence for the effect of electronic band structure on nonstoichiometry behavior. J Solid State Chem. 1997;133(2):555–67. DOI: 10.1006/jssc.1997.7531

[49] Adler SB. Factors governing oxygen reduction in solid oxide fuel cell cathodes. Chem Rev. 2004;104(10):4791–844. DOI: 10.1021/cr020724o

[43] Carter S, Selcuk A, Chater RJ, Kajda J, Kilner JA, Steele BCH. Oxygen transport in selected nonstoichiometric perovskite-structure oxides. Solid State Ionics. 1992;53–56, Part 1(0):597–605. DOI: 10.1016/0167-2738(92)90435-R

[50] Adler S, Russek S, Reimer J, Fendorf M, Stacy A, Huang QZ, et al. Local-structure and oxide-ion motion in defective perovskites. Solid State Ionics. 1994;68(3–4):193–211. DOI: 10.1016/0167-2738(94)90177-5

[44] Tanasescu S, Totir ND, Marchidan DI. Thermodynamic properties of some perovskite type oxides used as SOFC cathode materials. Solid State Ionics. 1999;119(1–4):311–5. DOI: 10.1016/S0167-2738(98)00520-7

[51] Hagenmuller P, Pouchard M, Grenier JC. Nonstoichiometry in the Perovskite-type oxides - an evolution from the classical Schottky-Wagner model to the recent high-Tc Superconductors. Solid State Ionics. 1990;43:7–18. DOI: 10.1016/0167-2738(90)90464-3

[45] Fisher CAJ, Yoshiya M, Iwamoto Y, Ishii J, Asanuma M, Yabuta K. Oxide ion diffusion in perovskite-structured $Ba_{1-x}Sr_xCo_{1-y}Fe_yO_{2.5}$: A molecular dynamics study. Solid State Ionics. 2007;177(39–40):3425–31. DOI: 10.1016/j.ssi.2006.03.060

[46] Wessel C, Lumey MW, Dronskowski R. First-principles electronic-structure calculations on the stability and oxygen conductivity in $Ba_{0.5}Sr_{0.5}Co_{0.8}Fe_{0.2}O_{3-\delta}$. J Membrane Sci. 2011;366(1–2):92–6. DOI: 10.1016/j.memsci.2010.09.046

[47] Girdauskaite E, Ullmann H, Al Daroukh M, Vashook V, Bulow M, Guth U. Oxygen stoichiometry, unit cell volume, and thermodynamic quantities of perovskite-type oxides. J Solid State Electr. 2007;11(4):469–77. DOI: 10.1007/s10008-006-0175-2

[48] Attaoua M, Beriala S, Omari M. Defect chemistry and physical